Mol Neurobiol (2009) 40:157–165
DOI 10.1007/s12035-009-8078-8

The Modulation by Intensity of the Processing of Interaural Timing Cues for Localizing Sounds

Eri Nishino · Harunori Ohmori

Received: 15 April 2009 / Accepted: 30 June 2009 / Published online: 11 July 2009

Abstract Features of sounds such as time and intensity are important binaural cues for localizing their sources. Interaural time differences (ITDs) and interaural level differences are extracted and processed in parallel by separate pathways in the brainstem auditory nuclei. ITD cues are small, particularly in small-headed animals, and processing of these cues is optimized by both morphological and physiological specializations. Moreover, recent observations in mammals and in some birds indicate that interaural time and level cues are not processed independently but cooperatively to improve the detection of interaural differences. This review will specifically summarize what is known about how inhibitory circuits improve the measurements of ITD in a sound-level-dependent manner.

Keywords Sound localization · Interaural time difference · Sound intensity · Nucleus laminaris · Nucleus magnocellularis · Superior olivary nucleus · Coincidence detection

Introduction

The brain uses features of sounds for localizing their sources. The frequency content (spectrum), intensity, and temporal fine structure are captured in the cochlea, transformed to trains of action potentials in the tuned array of auditory nerve fibers, and then transmitted to auditory nuclei in the brainstem. In the brainstem, features of sounds, including time and intensity, are processed separately in parallel as cues for localizing sound sources [1–6]. Interaural comparisons of time [6–10] and level [11, 12] are both important cues for sound source localization in the owl. These two cues seem to be integrated first in the lateral shell of the central nucleus of the inferior colliculus [13, 14]. In the owl, a map of auditory space is generated in the external nucleus of the inferior colliculus [15, 16]. However, recent observations in mammals and birds indicate that time and intensity information are not processed independently but rather cooperatively to enhance the contrast of interaural difference cues even at the first stage of processing of these cues in the brainstem auditory nuclei [17, 18]. In this review, we will first summarize what is known about the neural mechanisms that enable accuracy in detecting coincident synaptic inputs, which is central to assessing ITD, and then review observations on how the intensity of sounds modulates the processing of ITD in birds and in mammals. We will concentrate on observations in birds here because studies in mammals have been reviewed comprehensively elsewhere [6, 19, 20]. Important recent observations in mammals are specializations such as the graded expressions of Kv1 channels along the tonotopic axis in lateral superior olive in rat [21] and the refinement of glycinergic receptor expressions on soma in medial superior olive in adult gerbil, opossum, rat, and bat [22]. These observations are consistent with the preceding report of synaptic terminal boutons housing flat vesicles on the cell soma and proximal dendrites in medial superior olive of cat [23].

Coincidence Detection as the Basis of Localizing Sound Sources

The frequency of sounds determines how accurately they can be localized. Although the range of audible frequencies

E. Nishino · H. Ohmori (✉)
Department of Physiology, Faculty of Medicine,
Kyoto University,
Kyoto 606-8501, Japan
e-mail: ohmori@nbiol.med.kyoto-u.ac.jp

varies among species, the precision is highest in the middle frequencies in most species [24, 25]. We focus here first on how this frequency dependence emerges by reviewing *in vitro* studies in birds.

Localization of sounds in the azimuth depends on the ability of neurons in nucleus laminaris (NL) to detect coincident input from the two ears in birds. NL receives timing signals from the each nucleus magnocellularis (NM; Fig. 1a). NM is a relay nucleus that extracts information about the fine temporal structure of sounds from auditory nerve fibers (ANF). In chickens, the projection to contralateral NL forms a delay line that could compensate for the ITD created outside of the head (Fig. 1c) [26]. Axons of NM neurons are myelinated. In the barn owl, the distance between nodes of Ranvier (internodal distance) was shorter within NL than outside of NL [8]. The short internodal distance is likely associated with slow conduction of spikes within the nucleus, enhancing the accuracy of coincidence detection of bilateral action potentials.

NL neurons appear to work by "cross-correlating" synaptic conductances from each NM. These neurons are sensitive only to frequencies close to their own characteristic frequency (CF). CF is a sound frequency at which auditory neurons have the lowest threshold. When inputs from each ear arrive in phase at NL, they add, but when they arrive completely out of phase, they cancel. Therefore, ITD-tuning curves measured in NL *in vivo* have a period that depends on the neuron's CF. However; the recording in *in vitro* slice preparation demonstrated a single peak of coincidence detection when stimulus interval between each projection from NM was varied.

Recordings from slices of the chicken NL have revealed that coincidence detection varies systematically with the tonotopy and with the shape of excitatory postsynaptic potentials (EPSPs). The precision of coincidence detection was found to be proportional to the time course of EPSP [27]. When two electrical stimuli with a varying time interval were applied to the bilateral inputs from NM, responses to the two stimuli were summed (Fig. 2a). When the intervals were short, EPSPs were summed to produce a suprathreshold response but when the intervals were longer, EPSPs remained subthreshold. The precision of coincidence detection was evaluated by comparing the time intervals that induced 50% maximal firing (time window; Fig. 2b). The time window was dependent on the CF of neurons. When NL was separated into three CF regions of high (higher than 2.5 kHz, located at the rostromedial region of NL), middle (1–2.5 kHz), and low (0.4–1 kHz, located at the caudolateral region of NL) [28], the average time window was the smallest in cells that were recorded in slices corresponding to the middle CF region (0.3 ms), followed by the high CF region (0.6 ms), and was most broad in the low CF region (1.7 ms; Fig. 2c) [29]. The time

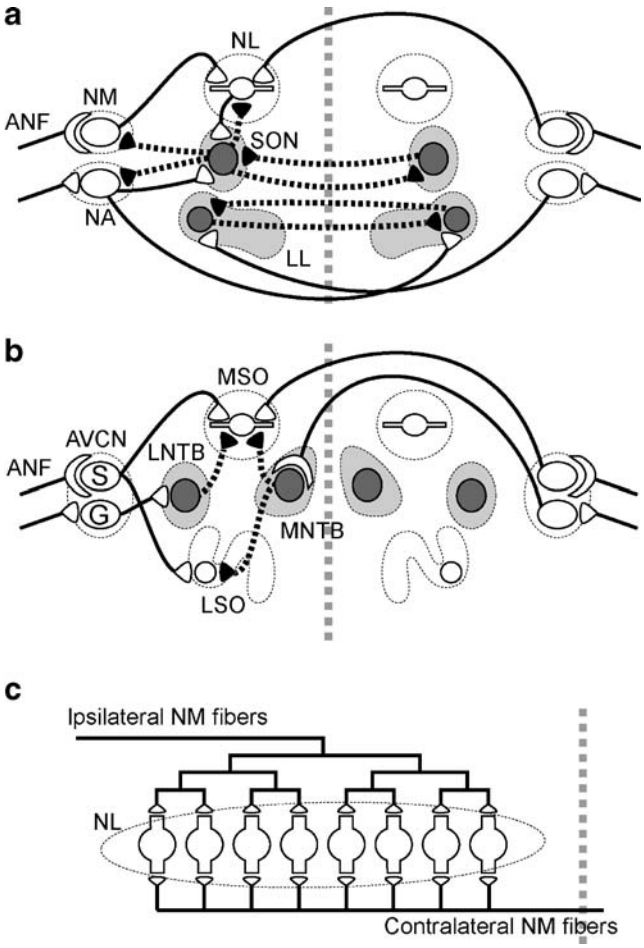

Fig. 1 Schematic diagrams of the auditory pathways for processing ITD and ILD in birds (**a**) and in mammals (**b**). The *vertical dotted line* represents the midline. See text for explanation. Note that both NL and medial superior olive make projections to higher-level auditory nuclei, and here, we summarized only the local circuits. **c** Modification of Jeffress model incorporating features of NL of the chick. The contralateral projections from NM to NL form delay lines. When a sound source moves toward more contralateral locations, spikes from contralateral NM will arrive at NL faster, and bilateral spikes arrive simultaneously at the NL neuron located more laterally

windows measured *in vivo* from single units in NL of the barn owl at the low (1–2 kHz), middle (3–5 kHz), and high (6–8 kHz) CF regions were approximately three times narrower than those of chickens *in vitro* but the pattern of dependence on CF was the same [8].

The time courses of excitatory postsynaptic currents (EPSCs) and EPSPs were studied in brain slices from the three CF regions of NL. EPSCs were prolonged in the low CF region [29]. The time course of EPSPs was the fastest in the middle CF region. Remarkably, in the middle CF region, EPSPs were not longer than EPSCs. The finding that dendrotoxin I prolonged the falling phase of the EPSPs indicated that dendrotoxin-sensitive K^+ channels abbreviate the falling phase of EPSPs [27]. Dendrotoxin I blocks low-voltage-activated K^+ channels that contain Kv1.1, Kv1.2,

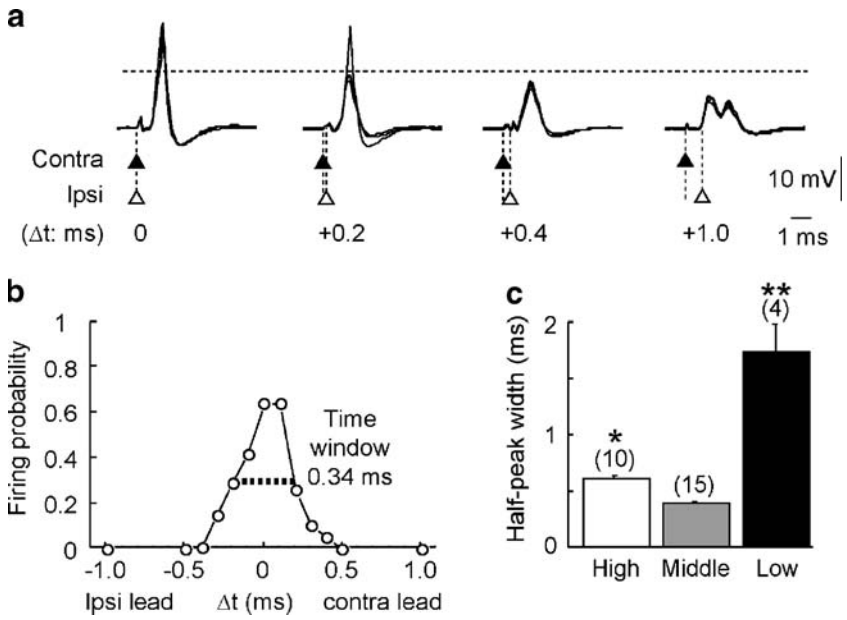

Fig. 2 Coincidence detection is most accurate in middle CF neurons. **a** Four superimposed voltage traces in response to bilateral stimuli at four different time intervals between the two sides (Δt in milliseconds, indicated in the figure, and positive value means that the contralateral stimulus precedes the ipsilateral stimulus; modified from Kuba et al. [27]). **b** Probability of spike generation as a function of Δt calculated from the neuron in **a**. The time window is indicated by the *horizontal broken line* (modified from Kuba et al. [27], Fig. 2Bc). **c** Time window plotted for three CF regions. *Numbers in parentheses* indicate the number of cells. $^{**}p<0.01$; $^{*}p<0.05$ (modified from Kuba et al. [29])

and Kv1.6 α subunits [30, 31]. NL expresses Kv1.2 differentially as a function of CF [29]. The expression level was the highest in the middle CF region of NL, followed by the high CF region, and was the lowest in the low CF region. This expression pattern of Kv1.2 channel was reciprocal to the distribution of the time window for coincidence detection and may largely determine the accuracy of coincidence detection in NL.

The frequency dependence of coincidence detection in slices has behavioral correlations in studies of sound localization [16, 32]. Most animals have the highest accuracy in the middle CF region within the hearing range inherent to that species. An interesting observation was made in the barn owl [33]. They used a short sound of 75 ms long and a long sound of 1 s long to test the accuracy of sound source localization. There was no difference in the error of localization at the initial stage of head orientation whether the test sound stimulus was short or long and whether the sound was a broadband noise or a pure tone. However, with a long sound stimulus, the barn owl adjusted the head orientation at the end of the stimulus, particularly for the test sounds emanating at an azimuthal angle more than 70° from the front. They concluded that the barn owl measures the ITD at the onset of sound. However, correcting the head orientation at the last stage of sound stimulus clearly improved the sound source localization error in the middle-high CF ranges (6–8 kHz) when a sound stimulus of 1 s long was used (Fig. 3 of Knudsen and Konishi [33]).

In the chicken NL, both HCN1 and HCN2 channels were found expressed along the tonotopic axis [34]. Expression of HCN1 depended robustly on the tonotopic axis and was higher in the low CF NL region, while the expression level of HCN2 was nearly constant across NL. HCN channels are activated by membrane hyperpolarization. Their voltage sensitivity is modulated by the cytosolic concentration of cyclic nucleotides [35]; their gating is shifted toward depolarized membrane potentials when the cytosolic cyclic nucleotide concentration is high. Dependency on cyclic nucleotide concentration is greater in HCN2 channels than in HCN1. NL cells depolarized when the level of cyclic AMP was raised either by incubation of slices with 8-Br-cAMP or photo-activation of the cell loaded with a caged compound of cyclic AMP, which likely reflected an increased activation of HCN channels at rest [34]. Membrane depolarization improved coincidence detection by accelerating the time course of EPSPs, presumably because of the consequent activation of low-voltage-activated K^+ channels. The relatively high density of HCN2 over HCN1 in the high CF region of NL made the high CF neurons more sensitive to the level of cyclic AMP. Moreover, incubation of slices prepared from the high CF region of NL with nor-adrenaline for a few minutes depolarized the neuron and made coincidence detection more sharp. Nor-adrenaline is a neurotransmitter released from sympathetic nerve terminals and is expected to activate G-protein-coupled receptors and increase cyclic AMP concentration in the target neurons [36]. These results raise the possibility that coincidence detection is under sympathetic control. The improved sound source localization in the middle to high frequencies of the barn owl [33] might be related to the sympathetic activity when the animal was exposed to a long sound stimulus. The expression pattern of HCN subunits has not been examined in owls, however.

Na channels on the axons of NL neurons, too, have a graded distribution that follows the tonotopic organization

[37]. Na channels are expressed in clusters on the first heminode of the axon. The cluster of Na channels lay distantly from the cell body in the higher CF regions of NL and closer to the soma in the lower CF regions of NL. At the lower CF regions, the cluster of Na channels also stretched over a longer distance. The somas of high CF, but not of low CF, neurons lacked Na channels. Axon initial segment changes with CF and myelinated in the higher CF neuron [38]. A simulation indicated that this distribution pattern of Na channels improved coincidence detection in a sound frequency-dependent manner [37, 39]. All these observations indicate that the distribution of ionic channels in NL is critically arranged to optimize sound source localization.

Precision of Timing Coding in NM

NM also has a tonotopic gradient in the expression of Kv1.1 channels [40]. The density of Kv1.1 was higher in the higher CF region of the nucleus than in the lower CF region. The high density of Kv1.1 increased the current required to activate spikes in the cell. NM neurons also demonstrated tonotopic gradients in the resting potential, spike threshold, and spike amplitude. The cells in the high CF region had more negative resting potentials, relatively more positive thresholds for action potentials, lower membrane resistances, and smaller spike amplitudes than those in the low CF region. In situ hybridization demonstrated the expression of mRNA for Kv1.2 in NM, which was not tonotopically graded; however, antibodies to Kv1.2 presently failed to detect protein expressions [40].

NM neurons do not have many dendrites and receive synaptic inputs of ANFs on the soma. Terminal arborizations of ANFs differed depending on the CF region (Fig. 3) [28, 40]. In the high-middle CF region of NM neurons (Fig. 3a), a small number of large end-bulbs of Held enfolded the cell [41–46]. However, in the low CF region, many small bouton-shaped terminals apposed NM neurons (Fig. 3b) [47]. The synaptic currents were graded along the tonotopic axis in slices [40]. Increasing the strength of stimuli to ANFs generated large EPSCs in an all-or-none manner in the high-middle CF region. The EPSCs generated suprathreshold EPSPs in NM neurons with action potentials that fired with invariant and precise (high-fidelity) timing following the spikes in ANFs [48]. However, in the low CF region, ANF generated small EPSCs that were graded with stimulus strength. In the low CF region, EPSPs were subthreshold, requiring the summation of inputs from multiple ANFs to cause NM neurons to fire. Summation of synaptic events was essential for a low CF NM neuron to be depolarized to threshold although the thresholds were lower than those of the high-middle CF cells because of the lower expression of Kv1.1 channels in low CF cells [40]. The low expression level of Kv channels also facilitates integration of temporally distributed synaptic events because of a longer membrane time constant.

The presence of many small synapses on low CF NM cells is advantageous for reducing temporal jitter in phase locked firing. Because the periods of sounds are longer, there is inherently more temporal jitter in the timing of ANF firing at low frequencies. In requiring the summation of subthreshold EPSPs in single, low CF NM cells, the temporal jitter in NM cells is reduced but still larger than in higher CF NM cells. The jitter of spike timing was found to be much smaller in low CF NM (lower than 800 Hz) than in ANF of similar CFs in the chicken (Fig. 3c) [49]. However, this improved phase locking in NM over ANFs was not found in the barn owl in CFs 1–10 kHz [50]. Improvement of spike timing was similarly reported in targets of ANFs in cats in the anteroventral cochlear

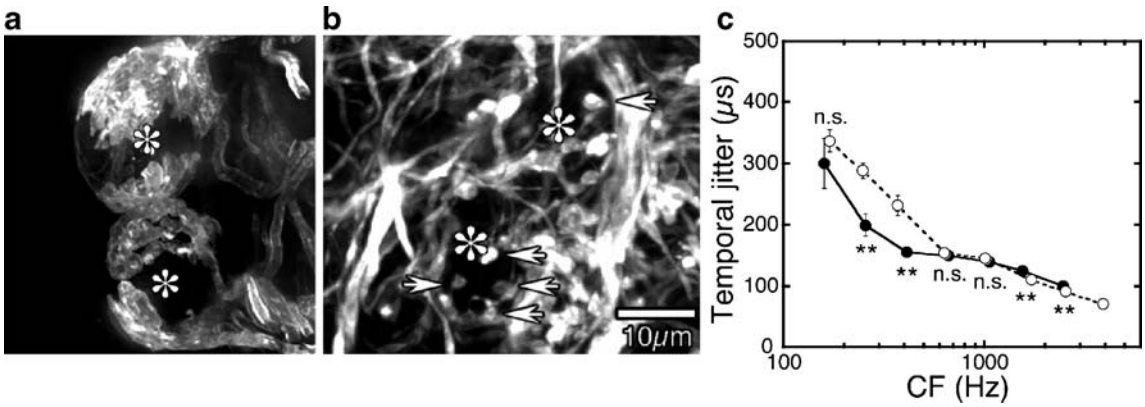

Fig. 3 Difference of terminal structures of ANFs along the CF axis in NM. **a**, **b** Patterns of projection of DiI-labeled ANFs. *Calibration bar* in **b** also applies to **a**. **a** High CF region. Neurons were innervated by a few nerve endings, and the terminal was large in the shape of an end-bulb of Held, and it enfolded the neuronal soma (*asterisks*). **b** Low CF region. Large enfolding terminals were not found, but many bouton-shaped terminals (*arrows*) were observed on cell soma (from Fukui and Ohmori [40]). **c** Averaged temporal jitter of ANF and NM was plotted against CF (from Fukui et al. [49])

nucleus [51]. Therefore, relay neurons like those in the NM of birds and the anteroventral cochlear nucleus of mammals are not simply relaying the timing information from ANF to the following coincidence detector neurons, but are refining the timing information during synaptic integration, perhaps by a mechanism of synaptic coincidence detection. Computer simulations demonstrate that spike timing is improved by the summation of many small synaptic inputs [52].

These observations in NL and NM indicate that sound localization acuity is achieved by many steps in brainstem auditory nuclei, by tonotopic specializations both morphologically and physiologically, and in both presynaptic and postsynaptic neurons.

Modulation of ITD Tuning by Sound Level

Medial superior olive of mammals is similar to NL in birds and processes ITD by detecting coincident excitatory inputs from spherical bushy cells in the anteroventral cochlear nucleus on each side of the brain (Fig. 1b) [53]. Single unit recordings from the medial superior olive of gerbils revealed that glycinergic inhibition improved ITD processing for low-frequency sound [17]. Suppression of inhibition by the iontophoretic application of strychnine increased the firing rate of medial superior olive neurons and shifted the peak of ITD-tuning curves from contralateral-leading ITD to 0 ITD. Brand et al. [17] concluded that precisely timed inhibition from the contralateral ear via the medial nucleus of the trapezoid body precedes the excitatory input from that side and creates an effective delay in the excitatory response, which is essential for ITD coding [17]. The medial nucleus of the trapezoid body is a relay nucleus, which receives excitatory input from contralateral globular bushy cells in the anteroventral cochlear nucleus, projects ipsilaterally to medial and lateral superior olive, and is a potential source for sound pressure level-dependent inhibition (Fig. 1b) [54–56]. Also, note recent findings that the medial nucleus of the trapezoid body is not a simple relay and sign-converting nucleus but its outputs could be modulated through integration of both excitatory and inhibitory synaptic inputs [57, 58].

In birds, processing of ITDs in NL is affected by sound loudness. Loud sound was expected to reduce the contrast between the peak and trough of the ITD-tuning curve (peak-trough contrast) by simulation [59]. However, the peak-trough contrast was maintained rather than reduced at high sound pressure level in *in vivo* recordings from the barn owl [60]. Pena et al. proposed that inhibition from the superior olivary nucleus (SON) controls ITD tuning in NL, rendering it tolerant to sound pressure level [60] (Fig. 1a).

GABA-containing terminals, largely from the SON, were found around the soma and proximal dendrites of NL. The SON receives excitatory inputs from both ipsilateral nucleus angularis and NL and inhibitory inputs from the contralateral SON; it forms GABAergic projections to the ipsilateral NL, NM, and nucleus angularis [61–64] (Fig. 1a).

ITD tuning in the NL of the chicken is under sound pressure level-dependent control by SON [18]. By recording single unit activity in NL *in vivo*, ITD tuning was found to depend both on the frequency and on level of sounds [18]. In the following discussion, best frequency (BF) is used as an alternative to CF. BF and CF are both measures of the frequency dependence of units. The difference is that BF is the sound frequency at which the neuron generates spikes at the highest rate when tested by a constant sound pressure level, while CF is the frequency at which neurons are driven at the lowest sound pressure level.

All NL units demonstrated clear ITD tuning and a well-defined, sound pressure level-sensitive peak-trough contrast [18] (Fig. 4a, c). The peak-trough contrast in middle to high BF units (BF higher than 1 kHz) was maximal at intermediate sound pressure levels. The peak-trough contrast was practically lost when a very loud sound was applied (90 dB or louder sound; Fig. 4c, d). In low BF units (lower than 1 kHz), however, the peak-trough contrast became larger as the sound became louder and the maximum contrast was maintained high, even at the loudest sound levels (Fig. 4a, b). After electrical lesion of the SON, the peak-trough contrast of ITD-tuning curve collapsed at loud sound levels in low-BF NL neurons [18] (Fig. 4e, f). The peak-trough contrast of the low BF units after lesion of SON was similar to that of the middle-high BF units and was maximized at the intermediate sound pressure level (Fig. 4e, f). However, the level dependence of peak-trough contrast of middle-high BF neurons was not different from the control after the lesioning of SON. These observations demonstrated that the BF dependence of level-dependent ITD tuning reflects the BF dependence of SON control on ITD tuning. The pattern and density of the SON projection to NL is correlated with this BF dependence of the effect of the SON [18]. The GABAergic projection from SON to NL was robust in the low BF region of the nucleus but became less prominent toward the high BF region. We conclude, therefore, that the dense inhibitory projection from SON to NL regulates ITD tuning in NL [18].

How the inhibition from SON to NL could modulate ITD tuning was studied with a computer simulation that is based on a NEURON model of ITD tuning [18, 37]. Level-dependent inhibition from SON was included in the model as an inhibitory conductance proportional to the excitatory inputs. This simulation could reproduce a level dependence of ITD tuning in NL neurons (Fig. 5a).

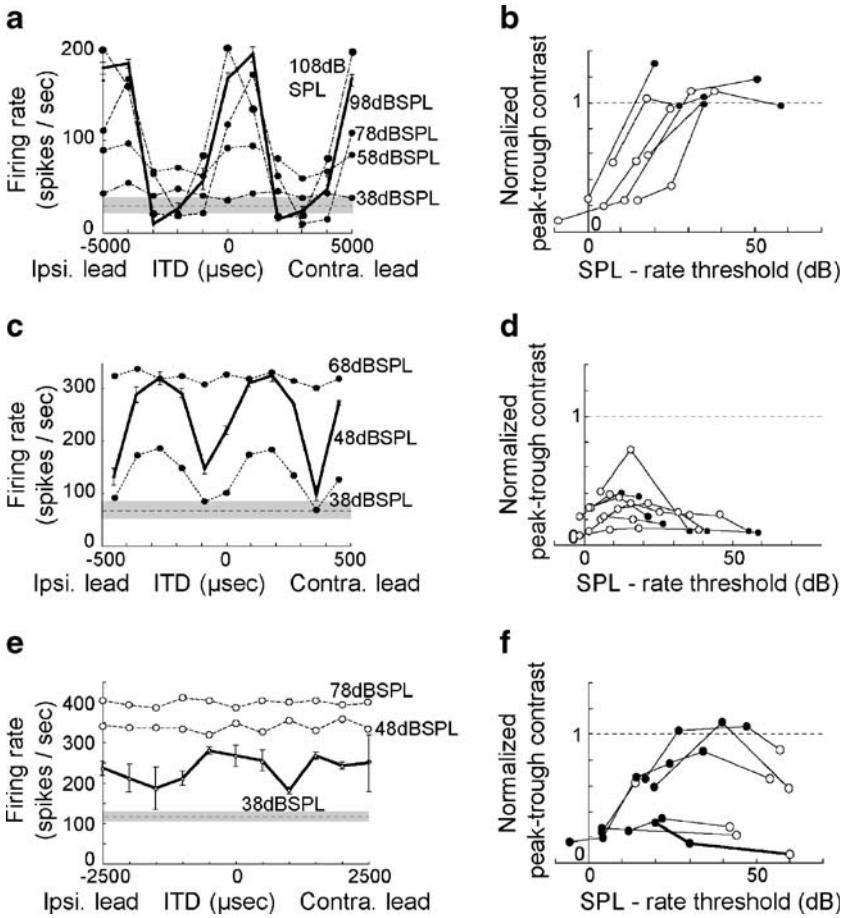

Fig. 4 ITD tuning to a pure-tone sound stimulus of best frequency in NL. **a**, **c**, **e** ITD-tuning curves. The *solid line with error bars of SEM* indicates the ITD-tuning curve of best peak-trough contrast, and the *horizontal broken line* and the *shade* indicate the mean ± SEM of spontaneous firing level. Stimulus SPL is indicated. **b**, **d**, **f** Normalized peak-trough contrast plotted against BF. A peak-trough contrast was defined as the difference in firing rates between the peak and the trough, normalized by the maximal firing rate of the unit after subtraction of the spontaneous firing rate. The symbols identify units. **a**, **b** A low BF neuron (200 Hz). **c**, **d** A middle-high BF neuron (2,400 Hz). **e**, **f** A low-BF neuron (400 Hz) after SON lesion (modified from Nishino et al. [18])

The SON receives sound intensity information from nucleus angularis and makes inhibitory projections to nucleus angularis, NM, and NL (Fig. 1a) [61, 63, 64]. We have discussed the role of inhibition from the SON to NL above; however, SON inhibition may also play a role in maintaining the balance of excitation from NM on the two sides. The simulation showed that without balanced bilateral excitation, the peak-trough contrast of

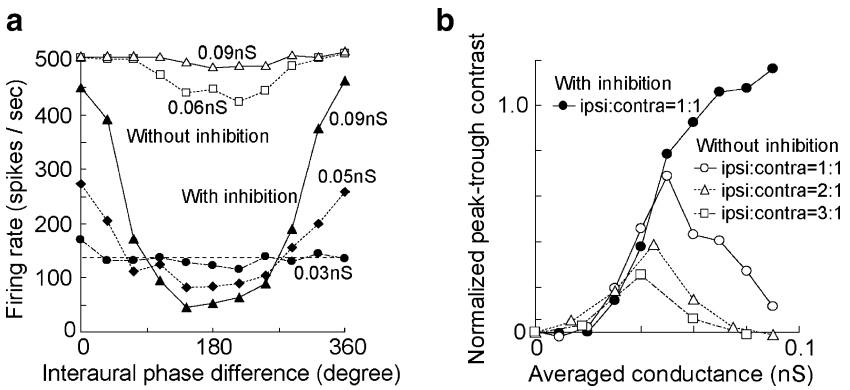

Fig. 5 Simulation of ITD responses for a low-BF NL neuron (500 Hz). **a** ITD-tuning curves were simulated for the control (*filled symbols*) and for the SON lesion (*open symbols*) conditions and plotted as a function of interaural phase difference. Averaged EPSP conductance is indicated. SON lesion was mimicked by setting the inhibitory conductance to zero and making the ipsilateral EPSP larger than the contralateral EPSP by a factor of 2. **b** Normalized peak-trough contrast as a function of averaged conductance of bilateral excitatory synaptic inputs, when inhibition was included (*filled symbols*) and inhibition was excluded (*open symbols*). *Different open symbols* indicate different levels of imbalance of EPSP conductance for contralateral to ipsilateral; 1:1 *open circles*; 1:2 *open triangles*; 1:3 *open squares* (modified from Nishino et al. [18])

ITD tuning lost tolerance to loud sounds [18] (Fig. 5b, open symbols). This simulation needs experimental proof, but agrees with the prediction by Dasika et al. [59], who made a computer model based on the assumption that SON activity might balance the effects of interaural intensity differences in processing ITD. Processing of ITD by NL was reported to be independent of interaural level difference (ILD) in the discharge rate, but the phase of spikes was affected by ILD in the barn owl [65]. Effects of ILD on the spike phase depended on the difference of the stimulus frequency relative to BF of the neuron and were not observed when frequency of sound stimuli matched the BF of the neurons. This effect was not likely mediated by SON activity and was interpreted to be a reflection of the physical properties of the inner ear [65].

Processing of ILD and ITD is complementary for localization of high- and low-frequency sounds, respectively (Duplex theory) [66–68]. The auditory system processes these two interaural difference cues by anatomically separate, physiologically distinct pathways [3, 69]. In recent years, evidence has accumulated that there are interactions between these two cues. In this review, we have shown that sound level affects the processing of ITD in chicken. It has also been shown that the processing of ILD in lateral superior olive depends critically on timing; the timing of contralateral inhibition through medial nucleus of the trapezoid body has to be matched with ipsilateral excitation [70–73].

Conclusion

Interaural difference cues can be small, particularly for an animal with a small head. We have reviewed here how the accuracy and precision of ITD processing is achieved and how ITD tuning is maintained over wide ranges in sound pressure level. We have summarized how the morphological specializations complement the roles of ionic channels in ITD tuning. New evidence suggests that timing and level of sounds are used cooperatively in both mammals and birds to improve the processing of small interaural cues.

Acknowledgments Authors acknowledge Dr. Donata Oertel for careful reading and useful comments on the manuscript. This work was supported by grants-in-aid (17023027) to HO.

References

1. Sullivan WE, Konishi M (1984) Segregation of stimulus phase and intensity coding in the cochlear nucleus of the barn owl. J Neurosci 4:1787–1799
2. Takahashi T, Moiseff A, Konishi M (1984) Time and intensity cues are processed independently in the auditory system of the owl. J Neurosci 4:1781–1786
3. Takahashi TT, Konishi M (1988) Projections of nucleus angularis and nucleus laminaris to the lateral lemniscal nuclear complex of the barn owl. J Comp Neurol 274:212–238
4. Warchol ME, Dallos P (1990) Neural coding in the chick cochlear nucleus. J Comp Physiol [A] 166:721–734
5. Moiseff A, Konishi M (1983) Binaural characteristics of units in the owl's brainstem auditory pathway: precursors of restricted spatial receptive fields. J Neurosci 3:2553–2562
6. Yin TC (2002) Neural mechamisms of encoding binaural localization cues in the auditory brainstem. In: e. Ortel D (ed) Integrative functions in the mammalian auditory pathway. Springer, New York, pp 99–159
7. Young SR, Rubel EW (1983) Frequency-specific projections of individual neurons in chick brainstem auditory nuclei. J Neurosci 3:1373–1378
8. Carr CE, Konishi M (1990) A circuit for detection of interaural time differences in the brain stem of the barn owl. J Neurosci 10:3227–3246
9. Overholt EM, Rubel EW, Hyson RL (1992) A circuit for coding interaural time differences in the chick brainstem. J Neurosci 12:1698–1708
10. Koppl C, Carr CE (2008) Maps of interaural time difference in the chicken's brainstem nucleus laminaris. Biol Cybern 98:541–559
11. Manley GA, Koppl C, Konishi M (1988) A neural map of interaural intensity differences in the brain stem of the barn owl. J Neurosci 8:2665–2676
12. Mogdans J, Knudsen EI (1994) Representation of interaural level difference in the VLVp, the first site of binaural comparison in the barn owl's auditory system. Hear Res 74:148–164
13. Takahashi TT, Wagner H, Konishi M (1989) Role of commissural projections in the representation of bilateral auditory space in the barn owl's inferior colliculus. J Comp Neurol 281:545–554
14. Takahashi TT, Konishi M (1988) Projections of the cochlear nuclei and nucleus laminaris to the inferior colliculus of the barn owl. J Comp Neurol 274:190–211
15. Knudsen EI (1983) Subdivisions of the inferior colliculus in the barn owl (Tyto alba). J Comp Neurol 218:174–186
16. Knudsen EI, Konishi M (1978) A neural map of auditory space in the owl. Science 200:795–797
17. Brand A, Behrend O, Marquardt T, McAlpine D, Grothe B (2002) Precise inhibition is essential for microsecond interaural time difference coding. Nature 417:543–547
18. Nishino E, Yamada R, Kuba H, Hioki H, Furuta T, Kaneko T, Ohmori H (2008) Sound-intensity-dependent compensation for the small interaural time difference cue for sound source localization. J Neurosci 28:7153–7164
19. Irvine R (1992) Physiology of the auditory brainstem. In: Popper AN, Fay RR (eds) The mammalian auditory pathway: neurophysiology. Springer, New York, pp 153–231
20. Oertel D (1999) The role of timing in the brain stem auditory nuclei of vertebrates. Annu Rev Physiol 61:497–519
21. Barnes-Davies M, Barker MC, Osmani F, Forsythe ID (2004) Kv1 currents mediate a gradient of principal neuron excitability across the tonotopic axis in the rat lateral superior olive. Eur J Neurosci 19:325–333
22. Kapfer C, Seidl AH, Schweizer H, Grothe B (2002) Experience-dependent refinement of inhibitory inputs to auditory coincidence-detector neurons. Nat Neurosci 5:247–253
23. Clark GM (1969) The ultrastructure of nerve endings in the medial superior olive of the cat. Brain Res 14:293–305

24. Klump GM, Windt W, Curio E (1986) The great tit's (Parus major) auditory resolution in azimuth. J Comp Physiol [A] 158:383–390
25. Brown C (1994) Sound localization. In: Fay RR, Popper AN (eds) Comparative hearing: mammals. Springer, New York, pp 57–96
26. Jeffress LA (1948) A place theory of sound localization. J Comp Physiol Psychol 41:35–39
27. Kuba H, Yamada R, Ohmori H (2003) Evaluation of the limiting acuity of coincidence detection in nucleus laminaris of the chicken. J Physiol 552:611–620
28. Rubel EW, Parks TN (1975) Organization and development of brain stem auditory nuclei of the chicken: tonotopic organization of n. magnocellularis and n. laminaris. J Comp Neurol 164:411–433
29. Kuba H, Yamada R, Fukui I, Ohmori H (2005) Tonotopic specialization of auditory coincidence detection in nucleus laminaris of the chick. J Neurosci 25:1924–1934
30. Robertson B, Owen D, Stow J, Butler C, Newland C (1996) Novel effects of dendrotoxin homologues on subtypes of mammalian Kv1 potassium channels expressed in Xenopus oocytes. FEBS Lett 383:26–30
31. Rathouz M, Trussell L (1998) Characterization of outward currents in neurons of the avian nucleus magnocellularis. J Neurophysiol 80:2824–2835
32. Klump G (2000) Sound localization in birds. In: Dooling RJ, Fay RR, Popper AN (eds) Comparative hearing: birds and reptiles. Springer, New York, pp 249–307
33. Knudsen EI, Konishi M (1979) Mechanisms of sound localization in the barn owl (Tyto alba). J Comp Physiol [A] 133:13–21
34. Yamada R, Kuba H, Ishii TM, Ohmori H (2005) Hyperpolarization-activated cyclic nucleotide-gated cation channels regulate auditory coincidence detection in nucleus laminaris of the chick. J Neurosci 25:8867–8877
35. Pape HC (1996) Queer current and pacemaker: the hyperpolarization-activated cation current in neurons. Annu Rev Physiol 58:299–327
36. Gilman AG (1987) G proteins: transducers of receptor-generated signals. Annu Rev Biochem 56:615–649
37. Kuba H, Ishii TM, Ohmori H (2006) Axonal site of spike initiation enhances auditory coincidence detection. Nature 444:1069–1072
38. Carr CE, Boudreau RE (1993) An axon with a myelinated initial segment in the bird auditory system. Brain Res 628:330–334
39. Ashida G, Abe K, Funabiki K, Konishi M (2007) Passive soma facilitates submillisecond coincidence detection in the owl's auditory system. J Neurophysiol 97:2267–2282
40. Fukui I, Ohmori H (2004) Tonotopic gradients of membrane and synaptic properties for neurons of the chicken nucleus magnocellularis. J Neurosci 24:7514–7523
41. Parks TN, Rubel EW (1978) Organization and development of the brain stem auditory nuclei of the chicken: primary afferent projections. J Comp Neurol 180:439–448
42. Whitehead MC, Morest DK (1981) Dual populations of efferent and afferent cochlear axons in the chicken. Neuroscience 6:2351–2365
43. Hackett JT, Jackson H, Rubel EW (1982) Synaptic excitation of the second and third order auditory neurons in the avian brain stem. Neuroscience 7:1455–1469
44. Carr CE, Boudreau RE (1991) Central projections of auditory nerve fibers in the barn owl. J Comp Neurol 314:306–318
45. Jhaveri S, Morest DK (1982) Sequential alterations of neuronal architecture in nucleus magnocellularis of the developing chicken: an electron microscope study. Neuroscience 7:855–870
46. Jhaveri S, Morest DK (1982) Sequential alterations of neuronal architecture in nucleus magnocellularis of the developing chicken: a Golgi study. Neuroscience 7:837–853
47. Koppl C (1994) Auditory nerve terminals in the cochlear nucleus magnocellularis: differences between low and high frequencies. J Comp Neurol 339:438–446
48. Brenowitz S, Trussell LO (2001) Minimizing synaptic depression by control of release probability. J Neurosci 21:1857–1867
49. Fukui I, Sato T, Ohmori H (2006) Improvement of phase information at low sound frequency in nucleus magnocellularis of the chicken. J Neurophysiol 96:633–641
50. Koppl C (1997) Phase locking to high frequencies in the auditory nerve and cochlear nucleus magnocellularis of the barn owl, Tyto alba. J Neurosci 17:3312–3321
51. Joris PX, Carney LH, Smith PH, Yin TC (1994) Enhancement of neural synchronization in the anteroventral cochlear nucleus. I. Responses to tones at the characteristic frequency. J Neurophysiol 71:1022–1036
52. Kuba H, Ohmori H (2009) Roles of axonal sodium channels in precise auditory time coding at nucleus magnocellularis of the chick. J Physiol 587:87–100
53. Goldberg JM, Brown PB (1969) Response of binaural neurons of dog superior olivary complex to dichotic tonal stimuli: some physiological mechanisms of sound localization. J Neurophysiol 32:613–636
54. Adams JC, Mugnaini E (1990) Immunocytochemical evidence for inhibitory and disinhibitory circuits in the superior olive. Hear Res 49:281–298
55. Spangler KM, Warr WB, Henkel CK (1985) The projections of principal cells of the medial nucleus of the trapezoid body in the cat. J Comp Neurol 238:249–262
56. Cant NB, Hyson RL (1992) Projections from the lateral nucleus of the trapezoid body to the medial superior olivary nucleus in the gerbil. Hear Res 58:26–34
57. Awatramani GB, Turecek R, Trussell LO (2004) Inhibitory control at a synaptic relay. J Neurosci 24:2643–2647
58. Lu T, Rubio ME, Trussell LO (2008) Glycinergic transmission shaped by the corelease of GABA in a mammalian auditory synapse. Neuron 57:524–535
59. Dasika VK, White JA, Carney LH, Colburn HS (2005) Effects of inhibitory feedback in a network model of avian brain stem. J Neurophysiol 94:400–414
60. Pena JL, Viete S, Albeck Y, Konishi M (1996) Tolerance to sound intensity of binaural coincidence detection in the nucleus laminaris of the owl. J Neurosci 16:7046–7054
61. Lachica EA, Rubsamen R, Rubel EW (1994) GABAergic terminals in nucleus magnocellularis and laminaris originate from the superior olivary nucleus. J Comp Neurol 348:403–418
62. Yang L, Monsivais P, Rubel EW (1999) The superior olivary nucleus and its influence on nucleus laminaris: a source of inhibitory feedback for coincidence detection in the avian auditory brainstem. J Neurosci 19:2313–2325
63. Monsivais P, Yang L, Rubel EW (2000) GABAergic inhibition in nucleus magnocellularis: implications for phase locking in the avian auditory brainstem. J Neurosci 20:2954–2963
64. Burger RM, Cramer KS, Pfeiffer JD, Rubel EW (2005) Avian superior olivary nucleus provides divergent inhibitory input to parallel auditory pathways. J Comp Neurol 481:6–18
65. Viete S, Pena JL, Konishi M (1997) Effects of interaural intensity difference on the processing of interaural time difference in the owl's nucleus laminaris. J Neurosci 17:1815–1824
66. Johnson DH, Dabak A, Tsuchitani C (1990) Function-based modeling of binaural processing: interaural level. Hear Res 49:301–319

67. Rayleigh L (1907) On our perception of sound direction. Philos Mag 13:214–232
68. Tsuchitani C, Johnson DH (1985) The effects of ipsilateral tone burst stimulus level on the discharge patterns of cat lateral superior olivary units. J Acoust Soc Am 77:1484–1496
69. Takahashi T, Konishi M (1986) Selectivity for interaural time difference in the owl's midbrain. J Neurosci 6:3413–3422
70. Joris PX, Yin TC (1995) Envelope coding in the lateral superior olive. I. Sensitivity to interaural time differences. J Neurophysiol 73:1043–1062
71. Smith PH, Joris PX, Yin TC (1993) Projections of physiologically characterized spherical bushy cell axons from the cochlear nucleus of the cat: evidence for delay lines to the medial superior olive. J Comp Neurol 331:245–260
72. Tollin DJ, Yin TC (2005) Interaural phase and level difference sensitivity in low-frequency neurons in the lateral superior olive. J Neurosci 25:10648–10657
73. Finlayson PG, Caspary DM (1991) Low-frequency neurons in the lateral superior olive exhibit phase-sensitive binaural inhibition. J Neurophysiol 65:598–605